

# NAD(P)H Oscillates in Pollen Tubes and Is Correlated with Tip Growth<sup>1</sup>

Luis Cárdenas\*, Sylvester T. McKenna, Joseph G. Kunkel, and Peter K. Hepler

Department of Biology and Plant Biology Graduate Program, University of Massachusetts, Amherst, Massachusetts 01003 (J.G.K., P.K.H.); Departamento de Biología Molecular de Plantas Instituto de Biotecnología, Universidad Nacional Autónoma de México, Morelos 62271, Mexico (L.C.); and Department of Biology, Long Island University, Brooklyn, New York 11201 (S.T.M.)

The location and changes in NAD(P)H have been monitored during oscillatory growth in pollen tubes of lily (*Lilium formosanum*) using the endogenous fluorescence of the reduced coenzyme (excitation, 360 nm; emission, >400 nm). The strongest signal resides 20 to 40  $\mu\text{m}$  behind the apex where mitochondria (stained with Mitotracker Green) accumulate. Measurements at 3-s intervals reveal that NAD(P)H-dependent fluorescence oscillates during oscillatory growth. Cross-correlation analysis indicates that the peaks follow growth maxima by 7 to 11 s or 77° to 116°, whereas the troughs anticipate growth maxima by 5 to 10 s or 54° to 107°. We have focused on the troughs because they anticipate growth and are as strongly correlated with growth as the peaks. Analysis of the signal in 10- $\mu\text{m}$  increments along the length of the tube indicates that the troughs are most advanced in the extreme apex. However, this signal moves basipetally as a wave, being in phase with growth rate oscillations at 50 to 60  $\mu\text{m}$  from the apex. We suggest that the changes in fluorescence are due to an oscillation between the reduced (peaks) and oxidized (troughs) states of the coenzyme and that an increase in the oxidized state [NAD(P)<sup>+</sup>] may be coupled to the synthesis of ATP. We also show that diphenyleneiodonium, an inhibitor of NAD(P)H dehydrogenases, causes an increase in fluorescence and a decrease in tube growth. Finally, staining with 5-(and-6)-chloromethyl-2',7'-dichloro-*fluorescein* acetate indicates that reactive oxygen species are most abundant in the region where mitochondria accumulate and where NAD(P)H fluorescence is maximal.

Pollen tube growth, which is essential for sexual reproduction in higher plants, is highly polarized and extremely fast (approximately 200–300 nm/s in lily [*Lilium formosanum*]; Hepler et al., 2001). In our quest to decipher the mechanism of growth, we have taken advantage of the fact that the growth rate oscillates, with changes in lily occurring from 100 to 500 nm/s during a period of 20 to 50 s. Because many of the underlying physiological processes also oscillate with the same period but not usually with the same phase and amplitude as growth, we have examined phase relationships using cross-correlation analysis to determine if a process precedes or follows growth (Holdaway-Clarke and Hepler, 2003). Anticipatory events are of particular interest because they may bear a more direct, causal role than following events in the growth regulatory mechanism.

Among the oscillatory processes, most attention has been directed toward ions, with the conclusion that chloride efflux mirrors growth rate (Zonia et al., 2002), whereas changes in intracellular and extracellular calcium, as well as extracellular protons and potassium, occur after growth (for review, see Holdaway-Clarke and Hepler, 2003). Especially with calcium, it has been unexpected to discover that this ion is a follower not a leader; its changes are predicted by the growth rate and not vice versa (Messerli et al., 2000; Holdaway-Clarke and Hepler, 2003). In our search for events that anticipate and potentially lead growth, we have turned our attention to metabolism, thinking that energy production and the processes that drive the synthesis of new cell wall material must at some level precede and anticipate the change in growth rate.

In this study, we focus on NAD(P)H in growing lily pollen tubes. These essential coenzymes occupy a central role in the control of cellular metabolism (Møller, 2001). Their high energy status and reducing power drive many key biosynthetic reactions and ATP production. Because NAD(P)H but not NAD(P)<sup>+</sup> possesses an endogenous fluorescence, it is possible to detect the reduced form in living cells; this property has been widely exploited (Lakowicz et al., 1992; Pogue et al., 2001; Schuchmann et al., 2001; Hu et al., 2002; Brachmanski et al., 2004; Blinova et al., 2005; Kasimova et al., 2006). Particularly pertinent are the oscillations in NADH that have been observed in yeast cells, which serve as a marker for changes in

<sup>1</sup>This work was supported by the National Science Foundation (grant nos. MCB-0055799 and MCB-0516852 to P.K.H.) and by Dirección General de Asuntas para el Personal Académico/Universidad Nacional Autónoma de México (grant no. IN-228903 and postdoctoral research to L.C.).

\*Corresponding author; e-mail [luis@ibt.unam.mx](mailto:luis@ibt.unam.mx).

The author responsible for distribution of materials integral to the findings presented in this article in accordance with the policy described in the Instructions for Authors ([www.plantphysiol.org](http://www.plantphysiol.org)) is: Luis Cárdenas ([luis@ibt.unam.mx](mailto:luis@ibt.unam.mx)).

[www.plantphysiol.org/cgi/doi/10.1104/pp.106.087882](http://www.plantphysiol.org/cgi/doi/10.1104/pp.106.087882)

metabolism (Ghosh and Chance, 1964; Goldbeter, 1996; Danø et al., 1999). In this study, we have examined changes in NAD(P)H during oscillatory pollen tube growth. We find that NAD(P)H oscillates with the same period as growth but not the same phase. Deconvolution of the signal reveals that at least one component, possibly NAD(P)<sup>+</sup>, anticipates changes in growth rate and thus might be a part of the central regulator of growth.

## RESULTS

### NAD(P)H Colocalizes with Mitochondria

When exciting at 360 nm and collecting the emission using a 400-nm long pass filter, we detect a fluorescent signal along the length of the pollen tube. Because these images are based on excitation and emission at single wavelengths, the amounts of fluorescence are not corrected for changes in optical path length. Nevertheless, by scanning a midline along the length of the tube, where the accessible volume will be relatively uniform, it becomes apparent that the signal is enriched in the apical 50  $\mu\text{m}$ , with the strongest component occurring about 20 to 40  $\mu\text{m}$  back from the apex, which corresponds to the base of the clear zone (Fig. 1, A and B). To provide further information about associated structures, we stained living cells with Mitotracker Green, a fluorescent dye that labels mitochondria. It can be seen in Figure 1 (C and D) that mitochondria, which occur along the length of the pollen tube, tend to accumulate in the region 20 to 40  $\mu\text{m}$  back from the apex. Line scan measurements along the length of the pollen tubes further indicate the close spatial localization of the NAD(P)H signal with the accumulation of mitochondria (Fig. 1, E and F).

### NAD(P)H Fluorescence Oscillates during Pollen Tube Growth Oscillation

Because pollen tubes of lily longer than 700  $\mu\text{m}$  reliably exhibit oscillations in their growth rate, we selected cells at this state of growth for the analysis of NAD(P)H fluorescence. Pollen tubes were thus repetitively excited by 360 nm light for 250 ms at 3-s intervals over a total time period of 10 min. Images from a segment of sequential data are shown in Figure 2; a graphic display of representative oscillations is shown in Figure 3. The resulting fluorescent signals clearly show distinct oscillations in which the peak fluorescence displays the same period as growth but not the same phase (Fig. 3). To provide more certainty on this point, we used autocorrelation to estimate the average periods of NAD(P)H titers and tip-growth rate within five independent pollen tubes; while the periods varied between 19 and 24.9 s between tubes, the periods of tip growth and NAD(P)H oscillation were virtually identical within tubes (data not shown). These oscillations in NAD(P)H fluorescence were not observed in

tubes that did not exhibit growth oscillations, e.g. pollen tubes starting to grow or terminating growth. Here, we only observe a constant signal in the subapical region (data not shown). We also determined that these oscillations in signal were not due to a nonspecific effect, such as changes in accessible volume. Thus, single wavelength measurements from cells loaded with rhodamine dextran, which fills the accessible cytoplasm and does not respond to ions (calcium or pH), failed to show an oscillatory pattern (data not shown).

To determine the phase relationship with growth, we subjected these data to cross-correlation analysis (Fig. 4). The results show that in the tip of the pollen tube, the NAD(P)H fluorescent peaks follow growth maxima by 7 to 11 s or 77° to 116°. However, the troughs in the data are also thought to contain important information. It is known, for example, that the strongest fluorescent signal derives from protein-bound NAD(P)H, whereas free NAD(P)H has a substantially weaker fluorescent signal (Wakita et al., 1995; Paul and Schneckenburger, 1996; Blinova et al., 2005). The oscillation, therefore, could arise from a change between bound and free forms. Alternatively, there could be an oscillation between reduced and oxidized forms, where the latter [NAD(P)<sup>+</sup>] is non-fluorescent. Accordingly, we looked at the negative view of these fluorescent traces in cross-correlation analysis. The results indicate that in the apical-most domain, the troughs anticipate peak growth by 5 to 10 s or 54° to 107°. In addition, the cross-correlation analysis reveals that the troughs are as strongly correlated with growth as are the peaks.

To increase our understanding of the spatial nature of this signal, we examined fluorescence in 10- $\mu\text{m}$  increments from a point centered at 5  $\mu\text{m}$  from the tip to a point centered at 55  $\mu\text{m}$  back using cross-correlation analysis of growth rate with regional NAD(P)H fluorescence (Fig. 4, B–G). In all areas, we are able to detect an oscillatory signal; however, the data show that the troughs are most advanced from growth at the extreme apex, with a gradual decline until 55  $\mu\text{m}$ , when the troughs are in phase with the growth rate (Fig. 4H). A similar analysis of the peaks reveals that they progressively fall further behind growth. Because each subarea of NAD(P)H measurement is being cross correlated with the same set of tip growth data, it is also evident that the apical areas of NAD(P)H fluorescence are most highly correlated with tip growth (Fig. 4, B–G); however, the strength of cross correlation progressively attenuates and reaches approximately 60% of the peak correlation at 55  $\mu\text{m}$  from the tip.

### Diphenyleneiodonium Increases NAD(P)H Fluorescence and Decreases Growth

To modify the levels of NAD(P)H and see how this affects both fluorescence and tube growth, we applied diphenyleneiodonium (DPI), which inhibits plasma

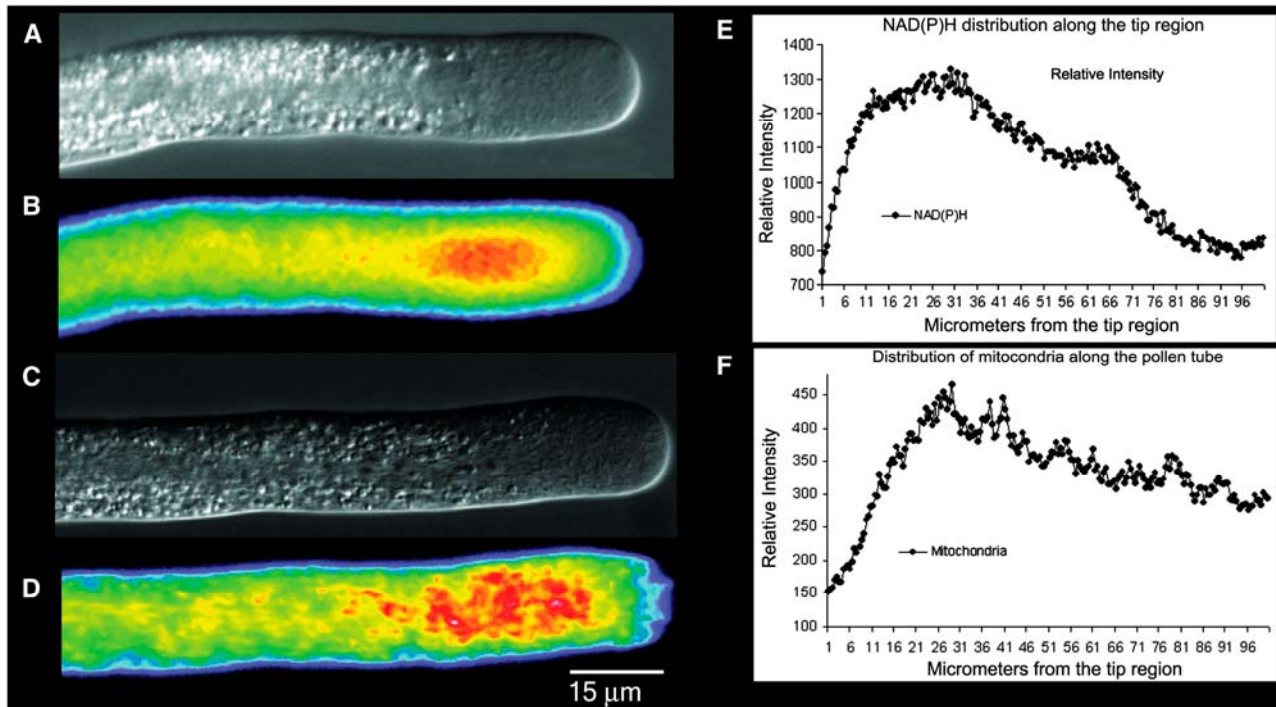


**Figure 1.** A and B, From the same pollen tube, the cell structure by DIC (A) and the distribution of NAD(P)H determined by its autofluorescence (B). Note the strongest signal at a region 20 to 40  $\mu\text{m}$  back from the apex. C and D, From another pollen tube, the DIC (C) image and the corresponding fluorescent image (D) revealing the distribution of mitochondria when stained with Mitotracker Green. Note the accumulation of mitochondria in the subapical region, 20 to 40  $\mu\text{m}$  back from the apex. In both B and D, the color follows convention, with red indicating high and blue indicating low levels of fluorescent signal. In E and F, a line scan along the length of the pollen tubes shown in B and D plots the distribution of NAD(P)H and mitochondria, respectively. Again, note the higher signal in the subapical region.

membrane NAD(P)H oxidases and mitochondrial NAD(P)H dehydrogenases and other flavoproteins (Roberts et al., 1995; Baker et al., 1998; Møller, 2001), to germinated pollen tubes that were exhibiting growth oscillations (Fig. 5). We first tested several different concentrations and found that 300  $\mu\text{M}$  caused a 50% growth inhibition. Higher concentrations (400, 500, and 625  $\mu\text{M}$ ) caused complete growth arrest or even tube bursting, whereas lower concentrations had no apparent effect (data not shown). With 300  $\mu\text{M}$  as the optimum concentration, we find that culture in DPI causes a relatively rapid 1.5- to 2-fold increase in total fluorescence, together with a concomitant 50% decrease in the pollen tube growth rate (Fig. 5, dashed line; white squares). Typically during the first 10 to 15 s after the addition of DPI, there is a noticeable but small increase in total fluorescence, followed in 20 to 60 s by a much larger increase (Fig. 5, solid line; black circles). The decline in growth rate does not begin immediately but only when the fluorescence reaches its maximum level; thereafter, the growth gradually slows (Fig. 5, dashed line; white squares trace).

### Reactive Oxygen Species Production Correlates Spatially with Mitochondrial Distribution

In other systems, notably, root hairs (Foreman et al., 2003), guard cells (Pei et al., 2000), and algal rhizoids (Coelho et al., 2002), interest has focused on a role for NAD(P)H in the generation of reactive oxygen species (ROS). Specifically, the oxidation of NAD(P)H has been associated with the formation of ROS, which are thought to play a signaling role that is central to polarized growth. To determine their status in pollen tubes, we stained the cells with 5-(and-6)-chloromethyl-2',7'-dichloro-*hydrofluorescein* acetate (CM-H<sub>2</sub>DCFDA), a fluorescent dye that has been used to detect ROS in other plant cells (Pei et al., 2000; Coelho et al., 2002), and then immediately microinjected the same pollen tube (less than 5 min) with the reference dye tetramethylrhodamine dextran (70 kD). Examination of ratio images reveals a region with high ROS production that is located in the subapical region at the base of the clear zone (Fig. 6, A and B). Although the extreme apex shows some ROS distribution, it is much less than in the subapical region (Fig. 6B; see asterisks).

This observation can be further confirmed from the line scan measurement, which indicates that the

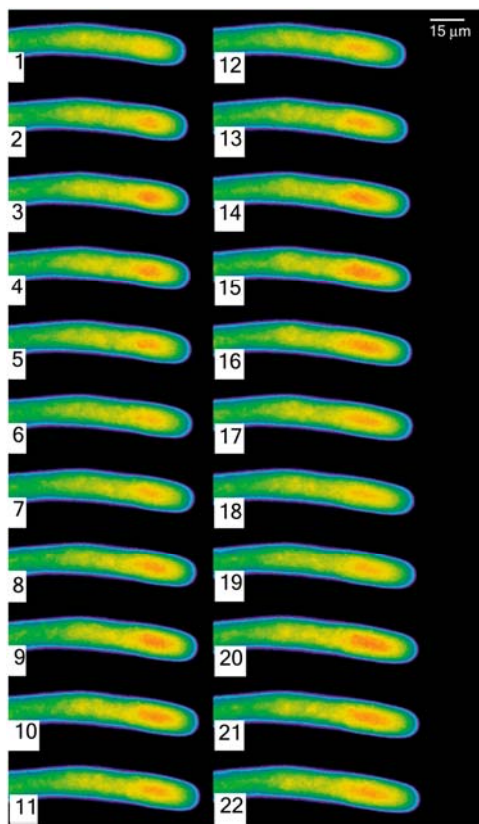


**Figure 2.** A time lapse sequence of a growing pollen tube reveals the changes in NAD(P)H fluorescence as the pollen tube grows. The individual images were acquired by exposure for 250 ms, with a 3-s interval between successive images. They are displayed in pseudocolor where red indicates high levels of NAD(P)H.

subapical region has an elevated level of ROS (Fig. 6C). Further studies involving a comparison of the ROS stain with Mitotracker Green reveal that the region with high ROS production correlates with the distribution of mitochondria and is largely excluded from the region of the inverted cone in the apex (compare Figs. 1D and 6B).

## DISCUSSION

The results show that the amount of NAD(P)H, based on its endogenous fluorescence, spatially correlates with the distribution of mitochondria (Fig. 1). Not only do we recognize that mitochondria are the major source of NAD(P)H in the cell, but the studies showing that the components of the glycolytic pathway are also associated with outer membrane of the mitochondria (Giegé et al., 2003) ensure that additional enzymes associated with NAD(P)H metabolism will be similarly localized. Although oxidation of NAD(P)H occurs at the plasma membrane in soybean (*Glycine max*) hypocotyls and even exhibits an oscillatory profile (Morré and Morré, 1998; Morré, 2004), this process will be only a fraction (10%) of that generated by mitochondria. In addition, the oscillatory

period for this process is 24 min and thus is 40 times longer than that reported herein in pollen tubes. We conclude, therefore, that mitochondrial metabolism accounts for the signal that we observe.

Of particular importance, the NAD(P)H-dependent fluorescence in pollen tubes oscillates and relates in a meaningful way to the corresponding oscillatory changes in the rate of growth (Figs. 2 and 3). When the signal is examined by cross-correlation analysis, the results indicate that the peak fluorescence follows the peak in growth rate. However, a similar analysis of the troughs indicates that they anticipate changes in growth rate (Fig. 4). A question that is often raised concerns how we can have confidence within an oscillatory context that an event either anticipates or follows changes in growth rate. To resolve this issue, we have used cross-correlation analysis, which permits us to establish the strength of covariance and lag between two processes, e.g. tip growth and process "x" (Brillinger, 1975). Because there are irregularities in the amplitudes, periods, and shapes of individual oscillation profiles, which are shared between tip growth and process "x", cross-correlation analysis is able to exploit those to establish the phase relationship. The direction of stronger correlation indicates the better fit and provides information on whether a process is phase advanced or retarded relative to growth rate. The process of cross-correlation analysis also provides information on the strength of fit, which can be important in helping us to determine which relationships are more meaningful.

Although the cross-correlation analysis indicates that the troughs and peaks are equal in their strength of correlation to growth, we focus on the troughs because they indicate a process that anticipates the changes in growth rate. It is our view that a preceding or anticipatory event may bear a closer relationship to the central regulator of growth than one that follows. The troughs represent a decrease in NAD(P)H fluorescence, which could be due to two different processes. First, it could be due to a shift from bound to free NAD(P)H in which the bound form exhibits a much stronger fluorescence than that which is free (Wakita et al., 1995; Paul and Schneckenburger, 1996; Blinova et al., 2005). Second, it could be due to oxidation of NAD(P)H, where the oxidized form [NAD(P)<sup>+</sup>] is nonfluorescent. Results from previously published studies appear to be in greater accord with the second option. Thus, Kasimova et al. (2006), using fluorescence lifetime spectroscopy, find a significant amount of free NADH in isolated potato (*Solanum tuberosum*) tuber mitochondria. Porcine heart mitochondria also contain substantial free (63%) NADH (Blinova et al., 2005). However, changes in the free component have not been detected. Wakita et al. (1995), in studies on rat liver mitochondria, report that the fluorescence signal is not due to changes in the environment (binding) but rather to changes in the amount of NAD(P)H. Kasimova et al. (2006) find that the concentration of free NADH in isolated po-

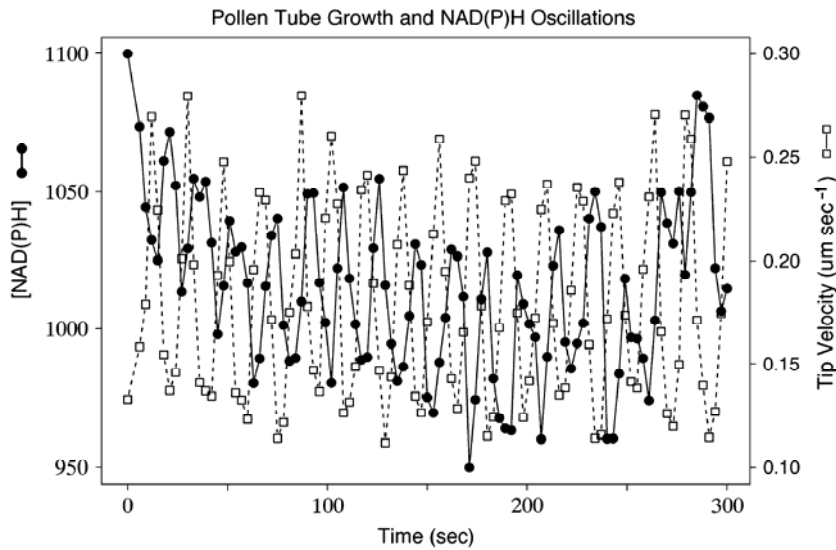


**Figure 3.** A comparison of the growth rate (dashed line; white squares), and NAD(P)H fluorescence, taken at about 20  $\mu\text{m}$  behind the tip (solid line; black circles), reveals that these two oscillatory signals show the same period but not the same phase.

tato tuber mitochondria remains constant, regardless of the metabolic conditions or the total amount of NADH. When taken together, these considerations lead us to favor the idea that the troughs in the oscillatory signal represent an increase in  $\text{NAD(P)}^+$ .

Of additional interest, the troughs are most advanced over growth in the apical domain, but they

become progressively less advanced in more basipetal regions until they are in phase with growth rate at about 50 to 60  $\mu\text{m}$  back from the tip (Fig. 4). Moreover, the troughs show a stronger correlation to growth rate in the apical domains where they are most advanced over growth rate. If the troughs represent a relative increase in  $\text{NAD(P)}^+$ , then the data in-

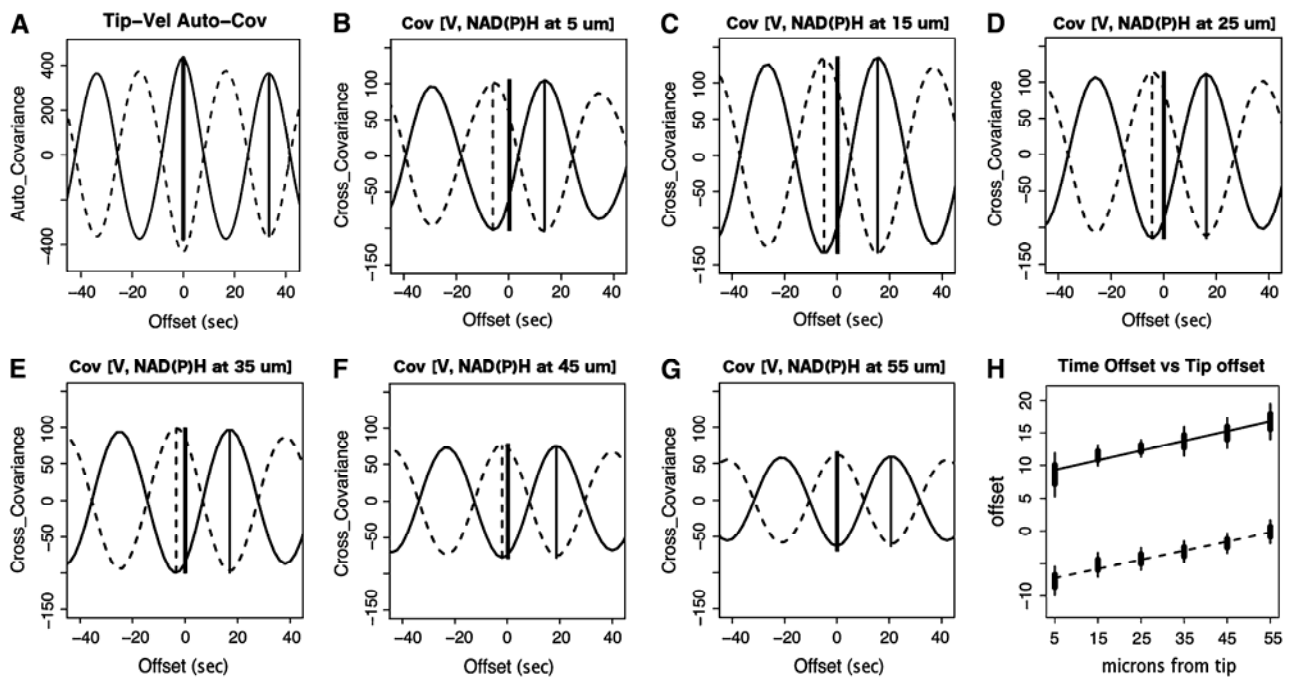
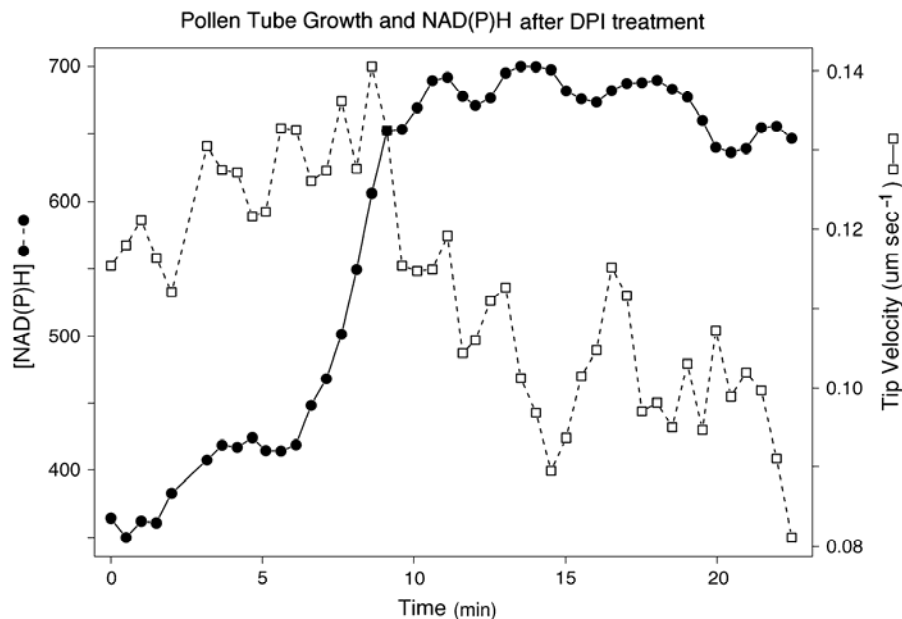


**Figure 4.** Cross-correlation analysis of tip growth with NAD(P)H fluorescence in incremental regions (10  $\mu\text{m}$ ) along the length of the pollen tube. A to G, Analysis of one pollen tube in a series of six. A, Autocorrelation of tip growth. The thick vertical bars represent 95% confidence intervals of the mean phase offset, while the thin vertical extensions mark 95% confidence intervals of the offsets. B to G, Cross covariance between tip growth and NAD(P)H fluorescence in circumscribed regions centered at 5, 15, 25, 35, 45, and 55  $\mu\text{m}$  behind the tip. The thick vertical solid line illustrates the position of zero offset. The displacement of the positive correlation peak is marked by a thin solid line and the displacement of the negative correlation is marked by a dashed vertical line. H, Average phase offset of NAD(P)H positive (solid line) and negative correlation (dashed line) of fluorescence to tip growth for the series of six tubes. The vertical bars represent a 95% confidence intervals of the mean phase offset.

**Figure 5.** Treatment of a pollen tube with DPI after 5 min of exposure causes a reduction in the growth rate (dashed line; white squares) and a concomitant increase in NAD(P)H autofluorescence (solid line; black circles).



dicating that the production of this oxidized species occurs first in the extreme apex and sets up a wave that spreads basipetally. The rearward propagation of the  $\text{NAD(P)}^+$  wave may represent the recharging of the coenzyme using resources that are posterior to the tip. Mitochondria, while lower in number relative to the subapical region, are nevertheless present very close to the tip (Fig. 1D; Lancelle and Hepler, 1992). It is possible that those mitochondria close to the growing tip are younger and more active than those located farther back. In support of this contention, we note a study on cultured chicken neurons, which shows that those mitochondria exhibiting a large membrane potential selectively move toward the actively extending growth cone (Miller and Sheetz, 2004).

Mitochondria extending close to the apex will also experience an oscillating calcium gradient (Holdaway-Clarke and Hepler, 2003), and this could influence metabolic processes. For example, three NAD(P)H dehydrogenases associated with the inner mitochondrial membrane are calcium-requiring enzymes (Møller, 2001). Oscillations in calcium would therefore be expected to induce an oscillation in the activity of these enzymes with an increase in calcium leading to a decrease in NAD(P)H (Michalecka et al., 2004). Current evidence reveals that the increase in cytoplasmic calcium at the apex follows changes in growth (Messerli et al., 2000); however, as shown herein, the decrease in NAD(P)H precedes growth by 5 to 10 s. A working hypothesis is that calcium may play a role in coordinating the activity of these enzymes, but as a following event it does not serve as the prime regulator. There are important unknowns that prevent us from developing this line of thought completely. Most importantly, while we know the temporal characteristics for the change in cytoplasmic calcium activity, we do not know if or

how those changes translate into calcium transients within the mitochondrion.

It is attractive to envision that the oxidation of NAD(P)H, yielding  $\text{NAD(P)}^+$ , is directly coupled to the synthesis of ATP, which is then used to power a variety of processes localized to the pollen tube apex. There could be many key steps that require ATP; however, we draw attention to a few events that are confined to the apical 10  $\mu\text{m}$  of the pollen tube. First, we note the internal alkaline band (Feijó et al., 1999), which presumably is generated by a proton-pumping ATPase located on the plasma membrane. The pumping of  $\text{H}^+$  creates a local gradient that likely affects the structure and activity of the nearby cortical actin fringe, as well as membrane transport activities. Second, actin polymerization, which favors G-actin bound with ATP, is essential for pollen tube elongation (Gibbon et al., 1999; Vidali et al., 2001) and participates in the formation of the prominent cortical actin fringe (Lovy-Wheeler et al., 2005). It is additionally pertinent that the dephosphorylation of F-actin ATP renders the filament sensitive to remodeling by the pH-sensitive actin-binding protein ADF (Blanchoin and Pollard, 1999). Third, both exocytosis and endocytosis take place at prodigious rates in the apex; these events are central to pollen tube elongation, and a need for ATP is evident (Parton et al., 2001; Camacho and Malhó, 2003). Finally, ATP is essential for kinases that phosphorylate and activate many essential enzymes needed for tip growth. We draw specific attention to nucleoside diphosphate kinase through which ATP can drive the synthesis of GTP. The formation of GTP is particularly important because it fuels the small G-proteins (Rops), which are located in the apex and play a central role in pollen tube growth (Hwang and Yang, 2006).

Additional results from this study underscore the relationship between NAD(P)H and growth, and em-

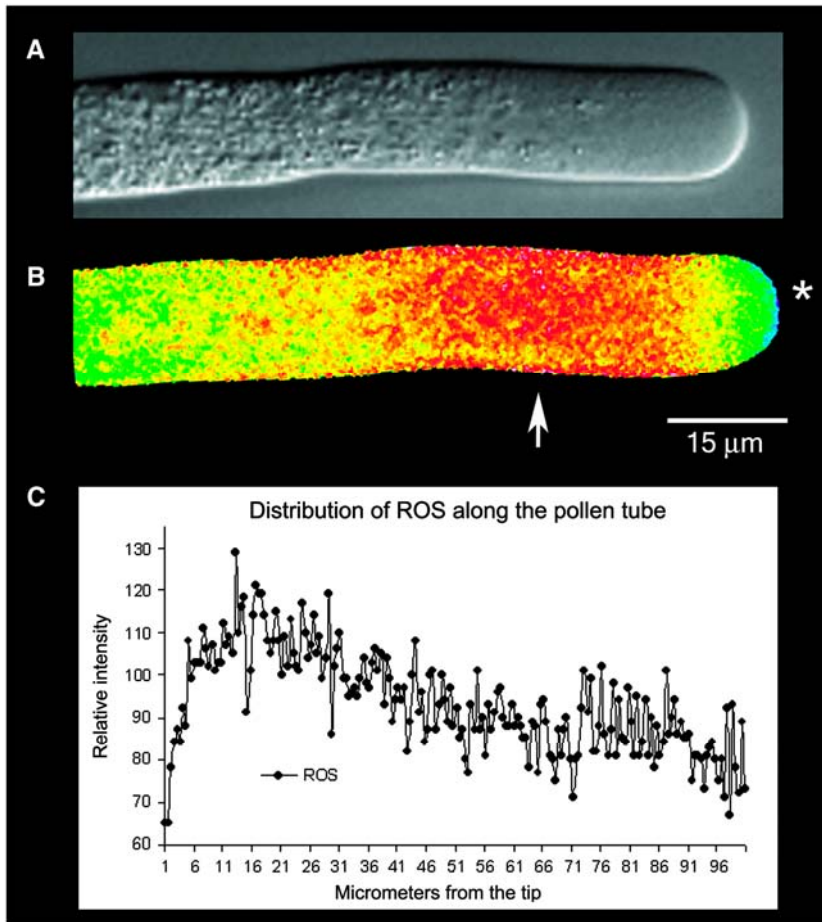


**Figure 6.** A and B show the same pollen tube. A, DIC image; B, fluorescence image indicating the relative distribution of ROS. To make this image, the pollen tube was microinjected with CM-H<sub>2</sub>DCFDA, which is sensitive to ROS, and tetramethyl-rhodamine 70 kD, which is an accessible volume marker. A ratio-image of the two fluorophores provides an indication of the distribution of ROS, which is independent of the optical path length. Note the highest values in the subapical region where mitochondria are more abundant (Fig. 1D). Figure 6C provides a line scan of intensity values along the length of the pollen tube shown in B. Note the increase in signal in the subapical region.

phasize the importance of achieving the correct balance between the oxidized and reduced forms of these coenzymes. Thus, the inhibition of NAD(P)H dehydrogenase activity with DPI leads to an increase in NAD(P)H and eventually to a decrease in the growth rate (Fig. 5). We also provide preliminary evidence about ROS production in pollen tubes. In agreement with several others (Pei et al., 2000; Murata et al., 2001; Coelho et al., 2002; Foreman et al., 2003), our studies are consistent with the idea that NAD(P)H is a prime participant. Staining the pollen tubes with CM-H<sub>2</sub>DCFDA reveals that ROS are most concentrated in the region where mitochondria accumulate and also where the NAD(P)H levels are most elevated (Fig. 6). A subapical, mitochondrial association with ROS production is also seen in tip-growing rhizoids of *Fucus* (Coelho et al., 2002). Despite these similarities, the *Fucus* rhizoid in addition shows a region of ROS production at the extreme apex that is not seen in pollen tubes. Although a certain amount of NAD(P)H oxidation may be coupled to the formation of ROS, which then serve a signaling role in guiding pollen tube growth, it seems likely that the bulk of NAD(P)H oxidation is coupled to cellular energetics, e.g. ATP synthesis.

In conclusion, we have shown that NAD(P)H fluorescence oscillates during oscillatory pollen tube

growth. Mathematical analysis of the phase relationship between NAD(P)H fluorescence and growth rate indicates that at least one component, possibly NAD(P)<sup>+</sup>, anticipates the changes in growth rate and might therefore occupy a position close to the central growth regulator. We favor the idea that oxidation of NAD(P)H with the concomitant production of ATP constitutes a primal event in pollen tube growth control. We also recognize that the NAD(P)H oxidation may be associated with formation of ROS and these may serve an important signaling function.

## MATERIALS AND METHODS

### Pollen Tube Growth

Pollen grains of lily (*Lilium formosanum*) were germinated and grown in lily growth medium (LGM), which is composed of 15 mM MES, 1.6 mM H<sub>3</sub>BO<sub>3</sub>, 1 mM KCl, 0.1 mM CaCl<sub>2</sub>, and 7% (0.2 M) Suc at pH 5.5. Pollen tubes were plated on a coverslip in an open glass slide chamber by mixing 35 μL of LGM containing the recently germinated pollen tubes and 35 μL of LGM, which contained 1.4% of low gelling point agarose (type VII; Sigma). This step turned out to be very critical as the layer of agarose on the coverslip should be as thin as possible to keep the pollen tubes flat and as close to the coverslip as possible. To ensure a thin layer, the coverslips were previously treated with hydrofluoric acid (5%) for 10 min, which slightly etched the glass and facilitated the tight binding of the agarose layer.

## NAD(P)H Detection

NAD(P)H is fluorescent and has been visualized by exciting at 340 to 365 nm and detecting emission at 400 to 500 nm (Lakowicz et al., 1992; Paul and Schneckenburger, 1996; Danø et al., 1999; Pogue et al., 2001; Schuchmann et al., 2001; Hu et al., 2002; Brachmanski et al., 2004; Blinova et al., 2005; Kasimova et al., 2006). To visualize the fluorescent signal, we used an inverted wide-field fluorescence microscope (Nikon TE-300), equipped with a CCD camera (CoolSnap HQ; Roper Instruments) mounted on the Köhler port, and a Xenon excitatory light source (DG-4; Sutter Instruments). Both the CCD camera and fluorescence light source were controlled by the MetaMorph/MetaFluor Image acquisition system (Universal Imaging).

Following experimentation with different filters on our microscope system, we found the best signal with the following setup: 360 nm (10-nm bandpass) as excitation filter, 380 nm dichroic, and 400-nm long pass emission filter (all filters from Chroma). Under these circumstances, the signal is evident and could be followed in living pollen tubes. Nevertheless, the signal is weak; therefore, we employed binning ( $2 \times 2$ ), which markedly increased the signal-to-noise ratio and allowed us to decrease the exposure time to 250 ms. These conditions permitted us to obtain a measurement every 3 s and thus to record fluorescence changes at multiple points during 5 to 10 min of oscillatory growth.

Because the above measurements of NAD(P)H were made at a single wavelength, we felt it was important to rule out nonspecific factors that could affect the signal. In particular, we were concerned about oscillatory changes in accessible volume because we had found in related studies that the endoplasmic reticulum displays a periodic movement in the apical domain during oscillatory pollen tube growth. To test for oscillations in accessible volume, we loaded pollen tubes with rhodamine dextran, an inert, space-filling dye, and measured its fluorescence changes in different regions of the tube during oscillatory growth.

## Mitochondrial Staining and ROS Measurements

For mitochondrial staining, we used Mitotracker Green (Molecular Probes), which was dissolved in LGM at a final concentration of  $2.5 \mu\text{M}$ . The pollen tubes were stained in the dye medium for 15 min, after which this medium was removed. The cells were rinsed once in LGM without dye and cultured in fresh LGM. Excitation was carried out at 495 nm, with fluorescence emission at 516 nm.

To detect ROS, we used CM-H<sub>2</sub>DCFDA (Molecular Probes). The stock dye was prepared at  $20 \mu\text{M}$  in dimethyl sulfoxide. A total of  $50 \mu\text{L}$  of this stock solution was applied to the growth chamber containing the pollen tubes for 20 min. Afterward, the cells were rinsed with dye-free medium and observed in the microscope. To obtain information about the relative changes in amount of ROS, we microinjected a reference dye (70 kD tetramethylrhodamine dextran; Molecular Probes) into pollen tubes previously loaded with CM-H<sub>2</sub>DCFDA. Image pairs were then acquired; first, we excited CM-H<sub>2</sub>DCFDA at 480 nm and collected the emission at 530 nm (ROS dependent), and, second, we excited tetramethyl-rhodamine dextran (70 kD) at 555 nm and collected the emission at 600 nm (ROS independent). A ratio of these two signals permitted us to map out the relative levels of ROS in the pollen tube.

## Inhibition of NADPH Oxidation

DPI is a general flavin dehydrogenase inhibitor; it has been used as an inhibitor of NAD(P)H oxidation (Roberts et al., 1995; Baker et al., 1998) and has been used to block root hair growth (Foreman et al., 2003). We prepared a stock solution of DPI (Sigma) at 25 mM in dimethyl sulfoxide. By using a peristaltic pump (Bio-Rad), we gradually replaced the original medium with one containing DPI at different concentrations. This approach avoids the physiological shock that can occur when the culture medium is suddenly removed with a pipette and quickly replaced with new medium.

## Oscillatory Phase Analysis Using Cross Correlation

Many physical and chemical phenomena in the pollen tube tip are convoluted in the four dimensions of space and time. We take a series of measurements as two-dimensional differential interference contrast (DIC) and fluorescence images and can isolate phenomena in those images as regions of pixels that identify the growing tip or an absorbance or fluorescence measure

of a chemical. These localized phenomena may be oscillating with varying periods and amplitudes, i.e. they are convoluted in ways the naked eye may not be able to discern. Deconvolution of the phenomena involves taking the recorded localized oscillations and mathematically reconvolving them in a pair-wise fashion to decide whether particular phenomena are changing with their own program, or if they are in concert with or phase-offset from another tube tip phenomenon. In this way, we are able to order the timing and spatial relations of events that occur in the tube tip.

Data were collected for growth and NAD(P)H fluorescence in 100 to 200 3-s bins with a DIC image plus a fluorescence image in each bin.

The DIC image, taken in 50 ms, produced the tip location, and those from adjacent bins were used to calculate growth rate, which was assigned to the mid-time between two successive DIC images. The fluorescence image was taken over a 1-s interval and assigned to a time midway through its collection. Fluorescence integrations were made in nonoverlapping,  $10\text{-}\mu\text{m}$  increments along the length of the tube.

For long-term effects on growth rate and fluorescence to be minimized, the data were normalized and smoothed (Cleveland, 1981) about a central trajectory. These operations provided a trace that oscillated about a zero baseline, allowing us to focus on the relationship of the oscillations. This is particularly useful for fluorescence data, which usually undergo a decline in signal due to bleaching during the course of the experiment.

We used cross-correlation analysis (Brillinger, 1975) to identify covarying events that are offset in time. In this approach, all phenomena are related to pollen tube growth rate, which is known to oscillate in a relatively regular pattern but with local variations in period and amplitude. These variations are critical; they help determine if a process precedes or follows growth and thus help in deciphering its phase relationship. In the first step, we performed an autocorrelation of growth rate. This identifies where a peak of zero offset would occur, and the nearest neighbor similar oscillation establishes a period from which phase offset relationships can be calculated. The period, which varies between 20 and 50 s, is then used to compute the phase offset of phenomena that is measured on the same pollen tube.

The convolve function (Brillinger, 1975) of R (Ihaka and Gentleman, 1996) is used here to compute an open mode convolution for the auto and cross covariance between growth rate and a paired phenomenon. (In the open mode of convolution, the data are padded at each end with zeroes and cross correlation is calculated with this zero padding as needed during offset of the compared data vectors.) The convolution procedure systematically computes the degree of covariance between two phenomena at different degrees of offset. In an autocorrelation, a maximum covariance of a phenomenon with itself is exhibited at zero offset. If the phenomenon is regular and periodic, additional peaks of covariance are located at the average wavelength of the periodic phenomenon. In our cross-correlation examples, the zero offset is marked by a solid black vertical line, and the peaks and troughs of covariance are offset left or right of this zero. The offset and height of the covariance peaks identify the phenomena that are most highly correlated with the growth rate. A convolution of the growth rate versus the positive and negative transform of NAD(P)H fluorescence allows us to determine its phase relationship to tip growth. Comparing convolutions of tip growth with NAD(P)H fluorescence of different regions provides the relative strengths of ties between those regions and tip growth.

Sequence data from this article can be found in the GenBank/EMBL data libraries under accession numbers ■■■■.

## ACKNOWLEDGMENTS

We thank Professor Max Møller, from The Royal Veterinary and Agricultural University, Frederiksberg, Denmark, for many helpful comments during the preparation of this study. We also thank our colleagues at University of Massachusetts for stimulating discussions.

Received August 16, 2006; accepted October 10, 2006; published ■■■■.

## LITERATURE CITED

Baker CJ, Deahl K, Domek J, Orlandi EW (1998) Oxygen metabolism in plant/bacteria interactions: effect of DPI on the pseudo-NAD(P)H oxidase activity of peroxidase. *Biochem Biophys Res Commun* **252**: 461–464



- Blanchoin L, Pollard TD** (1999) Mechanism of interaction of *Acanthamoeba* actophorin (ADF/Cofilin) with actin filaments. *J Biol Chem* **274**: 15538–15546
- Blinova K, Carroll S, Bose S, Smirnov AV, Harvey JJ, Knutson JR, Balaban RS** (2005) Distribution of mitochondrial NADH fluorescence lifetimes: steady-state kinetics of matrix NADH interactions. *Biochemistry* **44**: 2585–2594
- Brachmanski M, Gebhard MM, Nobiling R** (2004) Separation of fluorescence signals from  $\text{Ca}^{2+}$  and NADH during cardioplegic arrest and cardiac ischemia. *Cell Calcium* **35**: 381–391
- Brillinger DR** (1975) *Time Series: Data Analysis and Theory*. Holt-Rinehart, New York
- Camacho L, Malhó R** (2003) Endo/exocytosis in the pollen tube apex is differentially regulated by  $\text{Ca}^{2+}$  and GTPases. *J Exp Bot* **54**: 83–92
- Cleveland WS** (1981) LOWESS: a program for smoothing scatterplots by robust locally weighted regression. *Am Stat* **35**: 54
- Coelho SM, Taylor AR, Ryan KP, Sousa-Pinto I, Brown MT, Brownlee C** (2002) Spatiotemporal patterning of reactive oxygen production and  $\text{Ca}^{2+}$  wave propagation in *Fucus* rhizoid cells. *Plant Cell* **14**: 2369–2381
- Danø S, Sorensen PG, Hynne F** (1999) Sustained oscillations in living cells. *Nature* **402**: 320–322
- Feijó JA, Sainhas J, Hackett GR, Kunkel JG, Hepler PK** (1999) Growing pollen tubes possess a constitutive alkaline band in the clear zone and a growth-dependent acidic tip. *J Cell Biol* **144**: 483–496
- Foreman J, Demidchik V, Bothwell JHF, Mylona P, Miedema H, Torres MA, Linstead P, Costa S, Brownlee C, Jones JDG, et al** (2003) Reactive oxygen species produced by NADPH oxidase regulate plant cell growth. *Nature* **422**: 442–446
- Ghosh A, Chance B** (1964) Oscillations of glycolytic intermediates in yeast cells. *Biochem Biophys Res Commun* **16**: 174–181
- Gibbon BC, Kovar DR, Staiger CJ** (1999) Latrunculin B has different effects on pollen germination and tube growth. *Plant Cell* **11**: 2349–2363
- Giegé P, Heaslewood JL, Roessner-Tunali U, Millar AH, Fernie AR, Leaver CJ, Sweetlove LJ** (2003) Enzymes of glycolysis are functionally associated with the mitochondrion in *Arabidopsis* cells. *Plant Cell* **15**: 2140–2151
- Goldbeter A** (1996). *Biochemical Oscillations and Cellular Rhythms*. Cambridge University Press, Cambridge
- Hepler PK, Vidali L, Cheung AY** (2001) Polarized cell growth in higher plants. *Annu Rev Cell Dev Biol* **17**: 159–187
- Holdaway-Clarke TL, Hepler PK** (2003) Control of pollen tube growth: role of ion gradients and fluxes. *New Phytol* **159**: 539–563
- Hu Q, Yu ZX, Ferrans VJ, Takeda K, Irani K, Ziegelstein RC** (2002) Critical role of NADPH oxidase-derived reactive oxygen species in generating  $\text{Ca}^{2+}$  oscillations in human aortic endothelial cells stimulated by histamine. *J Biol Chem* **277**: 32546–32551
- Hwang JU, Yang Z** (2006) Small GTPases and spatiotemporal regulation of pollen tube growth. *Plant Cell Monogr* **3**: 95–116
- Ihaka R, Gentleman R** (1996) R<sup>!</sup>: a language for data analysis and graphics. *J Computat Graph Statist* **5**: 299–314
- Kasimova MA, Grigiene J, Krab K, Hagedorn PH, Flyvbjerg H, Andersen PE, Möller IM** (2006) The free NADH concentration is kept constant in plant mitochondria under different metabolic conditions. *Plant Cell* **18**: 688–698
- Lakowicz JR, Szmecinski H, Nowaczyk K, Johnson ML** (1992) Fluorescence lifetime imaging of free and protein-bound NADH. *Proc Natl Acad Sci USA* **89**: 1271–1275
- Lancelle SA, Hepler PK** (1992) Ultrastructure of freeze-substituted pollen tubes of *Lilium longiflorum*. *Protoplasma* **167**: 215–230
- Lovy-Wheeler A, Wilsen KL, Baskin TI, Hepler PK** (2005) Enhanced fixation reveals the apical cortical fringe of actin filaments as a consistent feature of the pollen tube. *Planta* **221**: 95–104
- Messerli MA, Creton R, Jaffe LF, Robinson KR** (2000) Periodic increases in elongation rate precede increases in cytosolic  $\text{Ca}^{2+}$  during pollen tube growth. *Dev Biol* **222**: 84–98
- Michalecka AM, Agius SC, Möller IM, Rasmusson AG** (2004) Identification of a mitochondrial external NADPH dehydrogenase by overexpression in transgenic *Nicotiana sylvestris*. *Plant J* **37**: 415–425
- Miller KE, Sheetz MP** (2004) Axonal mitochondrial transport and potential are correlated. *J Cell Sci* **117**: 2791–2804
- Möller IM** (2001) Plant mitochondria and oxidative stress: electron transport, NADPH turnover, and metabolism of reactive oxygen species. *Annu Rev Plant Physiol Plant Mol Biol* **52**: 561–591
- Morré DJ** (2004) Quinone oxidoreductases of the plasma membrane. *Methods Enzymol* **378**: 179–199
- Morré DJ, Morré DM** (1998) NADH oxidase activity of soybean plasma membranes oscillates with a temperature compensated period of 24 min. *Plant J* **16**: 277–284
- Murata Y, Pei ZM, Mori IC, Schroeder J** (2001) Abscisic acid activation of plasma membrane  $\text{Ca}^{2+}$  channels in guard cells requires cytosolic NAD(P)H and is differentially disrupted upstream and downstream of reactive oxygen species production in *abi1-1* and *abi2-1* protein phosphatase 2C mutants. *Plant Cell* **13**: 2513–2523
- Parton RM, Fischer-Parton S, Watahiki MK, Trewavas AJ** (2001) Dynamics of the apical vesicle accumulation and the rate of growth are related in individual pollen tubes. *J Cell Sci* **114**: 2685–2695
- Paul RJ, Schneckenburger H** (1996) Oxygen concentration and the oxidation-reduction state of yeast: determination of free/bound NADH and flavins by time-resolved spectroscopy. *Naturwissenschaften* **83**: 32–35
- Pei ZM, Murata Y, Benning G, Thomine S, Klusener B, Allen GJ, Grill E, Schroeder JI** (2000) Calcium channels activated by hydrogen peroxide mediate abscisic acid signalling in guard cells. *Nature* **406**: 731–734
- Pogue BW, Pitts JD, Mycek MA, Sloboda RD, Wilmot CM, Brandsema JF, O'Hara JA** (2001) In vivo NADH fluorescence monitoring as an assay for cellular damage in photodynamic therapy. *Photochem Photobiol* **74**: 817–824
- Roberts TH, Fredlund KM, Möller IM** (1995) Direct evidence for the presence of 2 external NAD(P)H dehydrogenases coupled to the electron-transport chain in plant-mitochondria. *FEBS Lett* **373**: 307–309
- Schuchmann S, Kovacs R, Kann O, Heinemann U, Buchheim K** (2001) Monitoring NAD(P)H autofluorescence to assess mitochondrial metabolic functions in rat hippocampal-entorhinal cortex slices. *Brain Res Brain Res Protoc* **7**: 267–276
- Vidali L, McKenna ST, Hepler PK** (2001) Actin polymerization is necessary for pollen tube growth. *Mol Biol Cell* **12**: 2534–2545
- Wakita M, Nishimura G, Tamura M** (1995) Some characteristics of the fluorescence lifetime of reduced pyridine nucleotides in isolated mitochondria, isolated hepatocytes, and perfused rat liver in situ. *J Biochem (Tokyo)* **118**: 1151–1160
- Zonia L, Cordeiro S, Tupy J, Feijó JA** (2002) Oscillatory chloride efflux at the pollen tube apex has a role in growth and cell volume regulation and is targeted by inositol 3,4,5,6-tetrakisphosphate. *Plant Cell* **14**: 2233–2249